Spc24 and Stu2 Promote Spindle Integrity When DNA Replication Is Stalled◻

Lina Ma,*† Jennifer McQueen,*† Lara Cuschieri,‡ Jackie Vogel,‡§ and Vivien Measday†

*Genetics Graduate Program and †Wine Research Centre/Michael Smith Laboratories, Faculty of Land and Food Systems, University of British Columbia, Vancouver, British Columbia, V6T 1Z4 Canada; and ‡Department of Biology and §Developmental Biology Research Initiative, McGill University, Montreal, QC, H3A 1B1 Canada

The kinetochore, a protein complex that links chromosomes to microtubules (MTs), is required to prevent spindle expansion during S phase in budding yeast, but the mechanism of how the kinetochore maintains integrity of the bipolar spindle before mitosis is not well understood. Here, we demonstrate that a mutation of Spc24, a component of the conserved Ndc80 kinetochore complex, causes lethality when cells are exposed to the DNA replication inhibitor hydroxyurea (HU) due to premature spindle expansion and segregation of incompletely replicated DNA. Overexpression of Stu1, a CLASP-related MT-associated protein or a truncated form of the XMAP215 orthologue Stu2 rescues *spc24-9* HU lethality and prevents spindle expansion. Truncated Stu2 likely acts in a dominant-negative manner, because overexpression of full-length *STU2* does not rescue *spc24-9* HU lethality, and spindle expansion in *spc24-9* HU-treated cells requires active Stu2. Stu1 and Stu2 localize to the kinetochore early in the cell cycle and Stu2 kinetochore localization depends on Spc24. We propose that mislocalization of Stu2 results in premature spindle expansion in S phase stalled *spc24-9* mutants. Identifying factors that restrain spindle expansion upon inhibition of DNA replication is likely applicable to the mechanism by which spindle elongation is regulated during a normal cell cycle.

INTRODUCTION

Preserving the integrity of the genome is a fundamental requirement for eukaryotic cell viability. DNA replication must be completed before segregation of the chromosomes to prevent the transmission of partially replicated chromosomes to daughter cells. In the budding yeast *Saccharomyces cerevisiae*, cells undergo a closed mitosis and the microtubule (MT) organizing centers, or spindle pole bodies (SPBs), are imbedded in the nuclear envelope. SPB duplication begins at the end of anaphase and spindle formation begins during S phase when duplicated SPBs separate from each other (Adams and Kilmartin, 1999; Jaspersen and Winey, 2004). Because chromosomes remain attached to kinetochore MTs throughout the cell cycle, spindle expansion must be restrained until all 16 chromosomes have duplicated and kinetochores on sister chromatids have formed bipolar MT attachments. When DNA replication is stalled by hydroxyurea (HU) treat-

ment, cells arrest with a large bud, an undivided nucleus positioned at the mother-bud neck and a short bipolar spindle (Allen *et al.*, 1994). Maintaining a short spindle is crucial for cell survival during HU-induced arrest, which activates the DNA replication checkpoint effectors Mec1 and Rad53 (Kolodner *et al.*, 2002). When *mec1* and *rad53* mutants are treated with HU, the DNA replication checkpoint is not activated, and, as a result, replication forks are not stabilized, the spindle expands, and unequal division of incompletely replicated nuclear material occurs—all of these events contribute to cell lethality (Allen *et al.*, 1994; Weinert *et al.*, 1994; Lopes *et al.*, 2001).

In human cells, stalled replication forks activate the ataxia telangiectasia mutated and Chk2 kinases, which are Mec1 and Rad53 homologues, respectively, and arrest the cell cycle by inhibiting mitotic entry (Canman, 2001). Until recently, it was presumed that *mec1* and *rad53* mutants enter mitosis prematurely upon HU treatment. However, two recent studies have shown that this is not the case, suggesting that spindle expansion is actively restrained when DNA replication is stalled (Krishnan *et al.*, 2004; Bachant *et al.*, 2005; Krishnan and Surana, 2005). Two mechanisms, which are not mutually exclusive, have been proposed for how spindle expansion is prevented during the DNA replication checkpoint. One mechanism suggests that spindle-associated proteins are regulated in a Mec1/Rad53-dependent manner (Krishnan and Surana, 2005). Spindle expansion and nuclear division of *mec1-1* mutants is reduced in cells carrying mutations of the kinesin-5/BimC orthologue Cin8 and XMAP215 orthologue Stu2 (Krishnan *et al.*, 2004). The second mechanism proposes that tension imposed by the bipolar attachment of kinetochores to MTs emanating from op-

posite SPBs is responsible for maintaining a short spindle upon inhibition of DNA replication (Bachant *et al*., 2005).

In budding yeast, each kinetochore, a multiprotein complex that resides on centromere (*CEN*) DNA, attaches to a single MT (McAinsh *et al*., 2003). After chromosome replication, kinetochores on sister chromatids must attach to MTs emanating from opposite SPBs to achieve bipolar attachment. The SPB pulling force opposes the cohesion holding sister chromatids together, and it creates tension that physically separates *CEN* regions during metaphase (Goshima and Yanagida, 2000; He *et al*., 2000; Pearson *et al*., 2001). The kinetochore not only attaches to spindle MTs but is also capable of regulating MT dynamics and spindle stability before and during mitosis. First, MT-associated proteins such as Stu2 and kinesin-related motor proteins localize to and function at kinetochores (He *et al*., 2001; McAinsh *et al*., 2003; Tanaka *et al*., 2005; Tytell and Sorger, 2006). Second, the Dam1 outer kinetochore complex encircles MTs, and mutations in Dam1 components severely affect MT dynamics (Cheeseman *et al*., 2001; Miranda *et al*., 2005; Westermann *et al*., 2005; Shimogawa *et al*., 2006). Third, a group of kinetochore proteins called chromosome passenger proteins relocalize from kinetochores to the spindle midzone during anaphase, and they regulate spindle stability and cytokinesis (Bouck and Bloom, 2005).

We have identified an HU-sensitive *spc24-9* kinetochore mutant that prematurely expands its spindle upon HU treatment. By performing a high copy suppressor (HCS) screen, we have identified 10 genes that when overexpressed rescue the HU sensitivity and spindle expansion defect of the *spc24-9* mutant strain. We characterized the rescue function of two of these genes—Stu1, a MT-associated protein that shares a region of similarity to the CLASP/Mast/Orbit subfamily of MT plus-end tracking proteins, and Stu2, a member of the conserved Dis1/XMAP215 family of MT plus-end binding proteins (Inoue *et al*., 2000; Yin *et al*., 2002; Gard *et al*., 2004). We demonstrate that both Stu1 and Stu2 are localized to the kinetochore early in the cell cycle and that Stu2 kinetochore binding depends on Spc24. By performing quantitative and time-lapse analysis of Stu2 fluorescence on spindles during HU treatment, we show that spindle expansion in *spc24-9* cells correlates with mislocalization of Stu2. We propose that localization of Stu2 to the kinetochore in cells when DNA replication is stalled is imperative for maintaining a short spindle and preventing separation of incompletely replicated DNA.

MATERIALS AND METHODS

Strain Construction

Standard methods for yeast culture and transformation were followed (Guthrie and Fink, 1991). Rich medium (YPD) and supplemental minimal medium (SC) were used (Kaiser *et al*., 1994) as well as FPM (minimal media supplemented with adenine and 6.5g/l sodium citrate) for microscopy analysis (Pot *et al*., 2005). Yeast strains used in this study are described in Supplemental Table S1. Genes were deleted or epitope tagged using standard yeast methods (Longtine *et al*., 1998).

HCS Screen

We transformed a 2μ yeast genomic DNA library carrying 6- to 8-kb genomic DNA fragments (Connelly and Hieter, 1996) into the *spc24-9* strain, and we plated 40,000 colonies onto SC-URA plates to select for the presence of the library plasmid. We then replica plated the colonies to 0.1 M HU (Sigma-Aldrich, Oakville, ON, Canada) SC-URA plates and incubated at 30°C to identify colonies that could rescue the HU lethality of *spc24-9* mutants. Library plasmids were rescued from colonies growing on the 0.1 M HU SC-URA plates and transformed back into *spc24-9* mutants to confirm the HU rescue phenotype. Plasmids were then sequenced using T3 and T7 primers to identify the flanking sequences of the genomic insert.

Plasmid Construction: Subcloning of HCS Genes

The coordinates of the genomic DNA identified in the HCS screen rescue plasmids and their subsequent subclones to confirm identity of the gene are as follows: *STU1ΔN*: Chr.II, 151363-158219; *STU1ΔN* subclone: Chr.II, 153753-158219; *STU2ΔN*: Chr.XII, 230442-237078; *STU2ΔN* subclone: Chr.XII 233569-237078; *KIP2*: Chr.XVI, 252390-259933; *KIP2* subclone: Chr.XVI, 257172-259933; *GIC1*: Chr.VIII, 220246-228530; *GIC1* subclone: Chr.VIII, 220246-222771; *RCK2*: Chr.XII, 634230-640397; *RCK2* subclone: Chr.XII, 634230-636611; *HCM1*: Chr.III, 224203-231351; *MCK1*: Chr. XIV, 52447-58767; *DMA1*: Chr.VIII, 337353-344031; *DMA1* subclone: Chr. VIII, 337353-342008. *DMA1* was confirmed as the gene responsible for rescue by digesting the *DMA1* subclone with EcoRI followed by Klenow treatment to create a frameshift in the *DMA1* gene. Full-length *MCK1* was a gift from Dr. Phil Hieter (University of British Columbia, Vancouver, BC, Canada) (Shero and Hieter, 1991), full-length *HCM1* was a gift from Dr. Trisha Davis (University of Washington, Seattle, WA) (Zhu *et al*., 1993), and full-length *STU1* and *STU2* were gifts from Dr. Tim Huffaker (Cornell University, Ithaca, NY) (Pasqualone and Huffaker, 1994; Wang and Huffaker, 1997).

Microscopic Analyses

Immunofluorescence. Cells shown or described in Figures 1, 3, 4, and 5 were imaged using a Zeiss Axioplan 2 microscope equipped with a CoolSNAP HQ camera (Photometrics, Tucson, AZ) and MetaMorph (Molecular Devices, Sunnyvale, CA) software. The indirect immunofluorescence microscopy studies in Figures 1 and 4 were performed as described previously (Hyland *et al*., 1999) with the following modifications. Cells were synchronized in G1 at 25°C by using 5 μg/ml α-mating factor (BioVectra, Charlottetown, Prince Edward Island, Canada), released into 0.2 M HU for 3 h at 30°C, and fixed with a final concentration of 3.7% formaldehyde for 1 h. Spindles were visualized by staining with Yol 1-34 rat anti-tubulin antibody (1:50) (Serotec, Oxford, United Kingdom) followed by fluorescein-conjugated goat anti-rat secondary antibody (1:2000). Single focal plane images were acquired with a 100× objective.

Analysis of Green Fluorescent Protein (GFP)-Centromeres, Stu1-VFP, and Stu2-VFP Localization in Fixed Cells. CEN15-GFP–tagged (Figure 3; Goshima and Yanagida, 2000) cells were synchronized with α-mating factor, and LacI-GFPHIS LacO::URA3-CEN15(1.8) was activated with 30 mM 3-aminotriazole in SC–HIS media. Cells were released into indicated concentrations of HU in FPM media for 3 h. Cells were washed and fixed in a total concentration of 4% paraformaldehyde for 15 min. Image stacks were acquired with a 100× objective at a step of 0.2 μm to span the entire cell. Stu1-VFP fluorescence (Figure 5) was imaged as described above for the following alterations. Cells were grown in FPM media at 30°C, synchronized with α-mating factor, and released to 30°C. After 30 min., samples were taken every 15 min and fixed in 70% ethanol. Stu2-VFP in fixed cells (Figure 7) was imaged with a WaveFX spinning disk confocal microscope (Quorum Technologies, Guelph, Ontario, Canada) as described previously (Cuschieri *et al*., 2006) without agar pads. Optical sections (0.5 μm) were acquired through a ±2.5-μm z-plane (total of 5.0-μm stack) by using Volocity 3DM acquisition software (Improvision, Conventry, United Kingdom).

Live Cell Analysis

For live-cell imaging of Stu2-VFP fluorescence intensities and spindle length measurements (Figure 8 and Supplemental Figure 3), overnight cultures were grown in YPD (containing 2× adenine sulfate) at 25°C to a cell density of ~0.3-0.4 OD$_{600}$ units ml^{-1}. Cultures were then diluted to 0.2 OD$_{600}$ units ml^{-1} and grown for an additional generation. Cells were arrested with 5 μg/ml α factor for 1.5 h at 25°C, washed, and then released into media containing 0.2 M HU for 1.5 h at 25°C. One-milliliter samples of each strain were taken and resuspended in ~50 μl of 30°C prewarmed media containing 0.2 M HU. Cells were mounted on a prewarmed 30°C heated stage and allowed to equilibrate for 15 min before imaging.

Multichannel four-dimensional imaging of Spc29-CFP and Stu2-VFP fluorescent fusion proteins was performed using a WaveFX spinning disk confocal system (Quorum Technologies) as described previously (Cuschieri *et al*., 2006). A Tokai Hit stage warmer was used to shift cells from 25 to 30°C, image acquisition commenced 15 min after the stage reached 30°C. Optical sections (0.5 μm) were acquired through a ±2.5-μm z-plane (total of 5.0-μm stack) at 2-min intervals for 30 min by using Volocity 3DM acquisition software (Improvision).

Spindle Length Measurements

Calculation of spindle lengths in fixed and live cell analyses shown in Figures 7 and 8 was performed using Volocity Classification (Improvision). Spindle lengths (in micrometers) were measured in triplicate for each time point, and the average value and SE of the mean determined. Lengths were determined by measuring the linear distance (micrometers; in x, y, z) between the midpoint of one SPB (Spc29-CFP channel) to the midpoint of the opposite SPB. All spindle lengths were measured in the XYZ plane view by using the line length

measurement tool. Average spindle lengths and SEs were calculated using Excel software (Microsoft, Redmond, WA).

Stu2-VFP Fluorescence Measurements

For Stu2-VFP fluorescence measurements shown in Figures 7 and 8, image stacks were acquired using an exposure of 91 ms/frame (providing an unsaturated image). For both fixed and live cell analyses, fluorescence intensity was measured by rastering a 4×4 voxel volume along the length of the long axis of the spindle (4×4 voxel: spindle fluorescent unit), including both SPBs. Background subtraction as performed as follows: the fluorescence in a 4×4 voxel volume positioned in the cytoplasm was measured, and subtracted from each fluorescence unit acquired along the spindle, resulting in corrected spindle fluorescence units (arbitrary units). For live cell analyses, background fluorescence was determined for each time point. The corrected fluorescence per unit length (fluorescence/micrometer) was calculated. Background subtractions, corrected fluorescence values, and standard deviations were calculated using Excel software.

Chromatin Immunoprecipitation (ChIP) Assays

ChIP experiments and primers used for polymerase chain reaction (PCR) analysis were performed as described previously (Measday *et al.*, 2002; Pot *et al.*, 2003). The linear range for PCR analysis was determined, and dilutions used for Figure 2A were total chromatin (T; 1:200), immunoprecipitation (IP; 1:1); for Figure 2B, T (1:200), IP (5:1); for and Figure 2C, T (1:200), IP (5:1). Dilutions used for Figure 6A were T (1:780), IP (1:6); for Figure 6B, T (1:780), IP (1:2.5); and for Figure 6, C and D, T (1:125), IP (1:1).

RESULTS

Spc24 Is Required for Viability and for Preventing Spindle Expansion during HU Arrest

The budding yeast Ndc80 central kinetochore complex, which is composed of the four coiled-coil proteins, Ndc80, Nuf2, Spc24, and Spc25, is required for proper attachment of chromosomes to spindle MTs and activation of the spindle checkpoint in the presence of defects in attachment (Janke *et al.*, 2001; Wigge and Kilmartin, 2001; Le Masson *et al.*, 2002; Montpetit *et al.*, 2005; Pinsky *et al.*, 2006). It has recently been shown that the kinetochore has a role in maintaining a short (1.5–2 μm) spindle when DNA replication is stalled by treatment of cells with HU (Bachant *et al.*, 2005). Previously, we created two mutants in the coiled-coil region of Spc24 (*spc24-8* and *spc24-10*) and one mutant in the C terminus of Spc24 (*spc24-9*) (Montpetit *et al.*, 2005). We tested these alleles for viability in the presence of HU at semipermissive temperature (30°C), and we found that the growth of the *spc24-9* mutant is sensitive to levels of HU that do not inhibit the growth of *spc24-8* and *spc24-10* mutants and the wild-type strain (Figure 1A). Next, we monitored the spindle length and bulk segregation of DNA in *spc24* mutants arrested in G1 and released into 0.2 M HU media. This analysis revealed that 100% of wild type and 98% of *spc24-8* and *spc24-10* mutants maintain a short spindle and undivided nuclei after 3-h exposure to HU; however, the majority (76%) of *spc24-9* mutants displayed elongated spindles and segregated nuclei (Figure 1, B and C). Our data suggest that the *spc24-9* mutation results in a defect in the function of the Ndc80 complex in preventing expansion of the spindle in cells with partially replicated DNA.

Characterization of the Kinetochore in spc24-9 Mutants

The Ndc80 complex is composed of two subcomplexes, Nuf2/Ndc80 and Spc24/Spc25, that are linked via their coiled-coil domains (Wei *et al.*, 2005). The C-terminal mutation in *spc24-9* lies within the Spc24 globular domain (Montpetit *et al.*, 2005; Wei *et al.*, 2005). To determine the state of the kinetochore and the Ndc80 complex in *spc24-9* mutants, we performed ChIP assays by using a member of the inner kinetochore CBF3 complex, Ndc10, and the Ndc80 protein. We found that Ndc10 was able to interact with centromere (*CEN*) DNA in *spc24-9* cells at both restrictive temperature (37°C) and
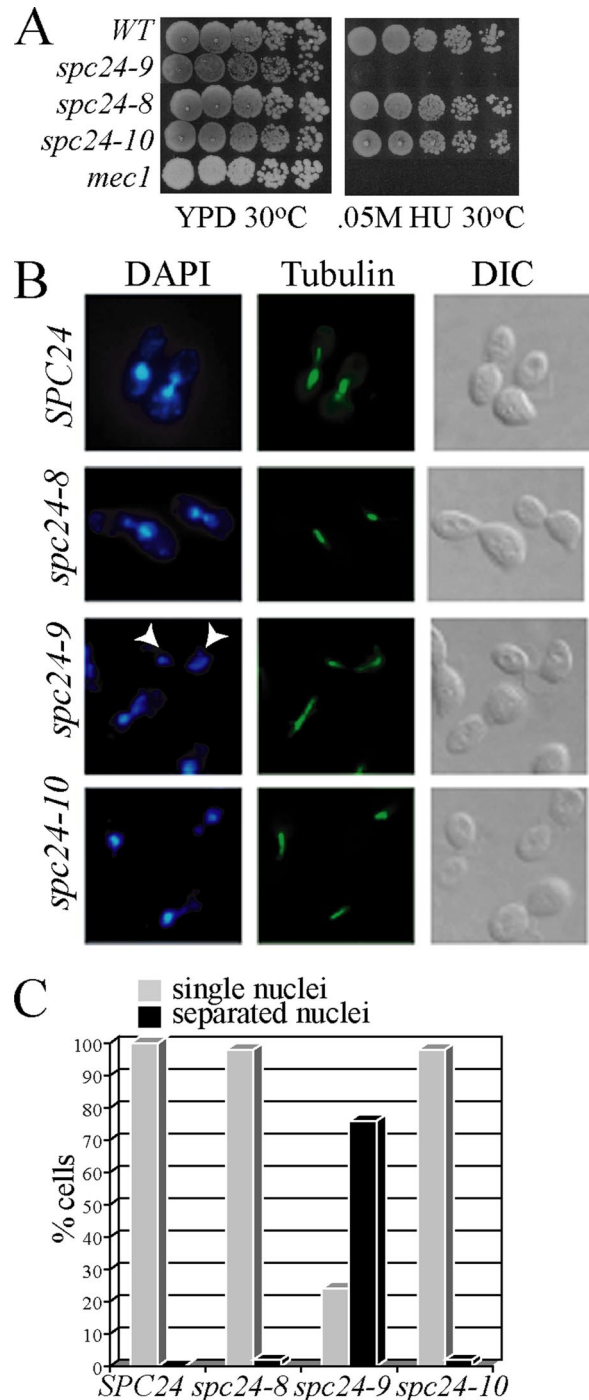
Figure 1. *spc24-9* mutants are sensitive to HU due to inappropriate spindle expansion. (A) Cell dilution assay of indicated strains grown on YPD and 0.05 M HU at 30°C for 3 d. (B) Immunofluorescence analysis of wild-type (*SPC24*), *spc24-8*, *spc24-9*, and *spc24-10* cells synchronized in G1 phase with α-factor and then released into 0.2 M HU for 3 h at 30°C. Shown are representative cells after 3-h HU treatment imaged for DNA (4,6-diamidino-2-phenylindole [DAPI]), MTs (tubulin) and cell morphology (differential interference contrast [DIC]). White arrowheads point to separated nuclei in the *spc24-9* mutant. (C) Percentage of cells (100 cells counted) described in B displaying single (gray bars) or separated (black bars) nuclei.
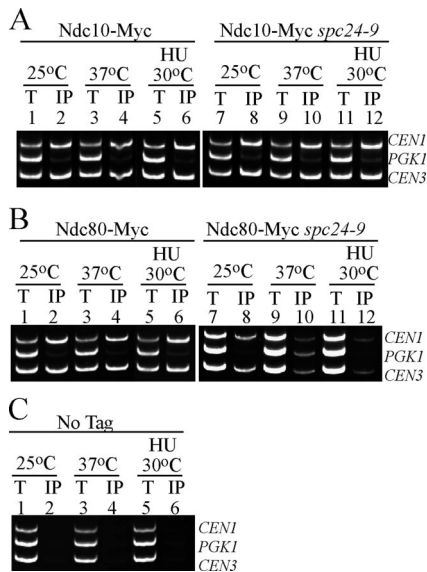
Figure 2. Ndc80 *CEN* association is disrupted in *spc24-9* mutants. Multiplex PCR analysis of *CEN1*, *PGK1*, and *CEN3* loci was performed with total chromatin (T) or immunoprecipitate (IP) as PCR templates. Strains were grown at 25°C to log phase and then either shifted to 37°C for 3 h or incubated in 0.2 M HU at 30°C for 3 h. (A) Ndc10-Myc wild type (lanes 1–6) or *spc24-9* cells (lanes 7–12). (B) Ndc80-Myc wild-type (lanes 1–6) or *spc24-9* cells (lanes 7–12). (C) Wild-type strain carrying no epitope tag (No Tag, lanes 1–6) shown as a control. An untagged *spc24-9* mutant was also used as a control and showed similar results (data not shown).

after 3 h of 0.2 M HU treatment at 30°C, suggesting that the core kinetochore is still intact in *spc24-9* mutants (Figure 2A, lanes 10 and 12). Ndc80, however, showed a clear defect in its ability to associate with *CEN* DNA in *spc24-9* cells both at 37°C and after 3 h of 0.2 M HU treatment at 30°C (Figure 2B, lanes 10 and 12). In corroboration with our ChIP data, we found that Ndc80-VFP localization was also perturbed in *spc24-9* mutants at 37°C and that it is even more affected in HU-arrested cells (Supplemental Figure 1). Eighty percent of HU-treated *spc24-9* mutants showed diffuse and weak Ndc80-VFP staining, suggesting that the Ndc80 complex is disrupted when *spc24-9* cells are exposed to 0.2 M HU (Supplemental Figure 1).

Bipolar Attachment Is Not a Requirement for Maintaining a Short Spindle in HU-treated Cells

Previous studies have suggested that specific kinetochore mutants display inappropriate spindle expansion during HU exposure due to their inability to establish kinetochore–MT bipolar attachment and thus appropriate tension on the spindle (Bachant *et al.*, 2005). Using a *CEN15*-GFP–marked strain, we found that a similar percentage of wild-type, *spc24-9*, and *spc24-10* cells displayed bipolar attachment in cells released from a G1 block to 30°C (Figure 3A). Thus, *spc24-9* kinetochores are capable of bipolar attachment to spindle poles during a normal cell cycle at the same temperature (30°C) that results in *spc24-9* HU lethality. Whether kinetochores attain bipolar attachment in a wild-type strain in the presence of partially duplicated DNA (as a result of treatment with HU) is unclear. We reasoned that exposing cells to increasing concentrations of HU would increase replication fork stalling (.05M-0.3M HU) and impact the number of *CEN*s that were replicated (Clarke *et al.*,
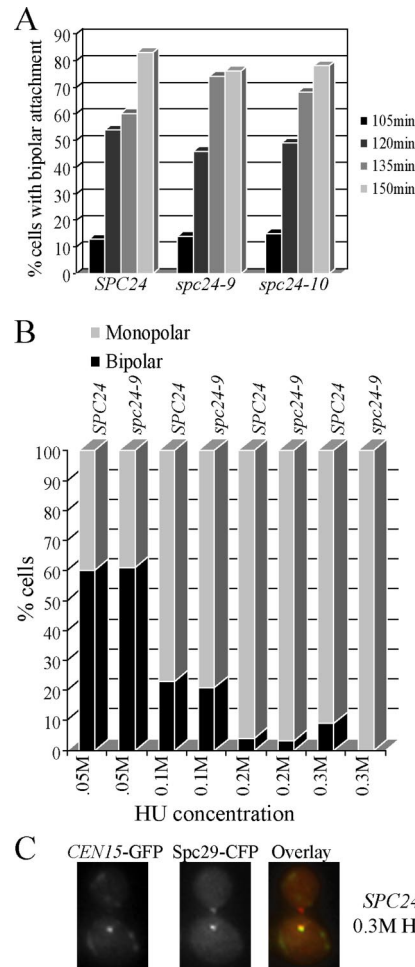
Figure 3. *spc24-9* mutants are capable of establishing bipolar attachment. (A) Wild-type (*SPC24*), *spc24-9*, and *spc24-10* strains carrying LacO repeats integrated 1.8 kb from *CEN15*, LacI-GFP, and Spc29-CFP were synchronized in G1 phase with α-factor and released at 30°C. Samples were taken every 15 min and imaged using fluorescence microscopy for the presence of the *CEN15*-GFP and Spc29-CFP signal. Shown are the time points (105 min onward) at which the cells began to display bipolar attachment (separation of *CEN15*-GFP signals). Duplicate experiments were performed with similar results. Shown is the result of one experiment in which 100 cells containing a spindle of 0.5 μm or larger were counted for each time point. (B) Wild-type (*SPC24*) and *spc24-9* *CEN15*-GFP Spc29-CFP strains were synchronized in G1 phase with α-factor, split into four cultures, and indicated concentrations of HU were added for 3 h at 30°C. Similar results were seen with duplicate experiments; thus, data from one experiment are shown (100 cells counted). (C) Example of a wild-type (*SPC24*) cell from B after 3 h of 0.3 M HU treatment that displays monopolar *CEN15* attachment. In the overlay, *CEN15*-GFP is green and Spc29-CFP is red.

2001). We monitored *CEN15* separation as a sign of bipolar attachment using *CEN15*-GFP and Spc29-CFP–tagged wild-type and *spc24-9* mutant strains. Wild-type cells treated with the lowest concentration of HU (0.05 M HU) exhibited *CEN15* bipolar attachment in 60% of cells after 3 h (Figure 3B). Importantly, *spc24-9* mutants displayed the same percentage of separated *CEN15* foci, suggesting once again, that *spc24-9* mutants are capable of bipolar attachment (Figure 3B). Similar to previous studies, we found that separated *CEN15* foci were detected in 23% of wild-type cells exposed to 0.1 M HU, yet only 4% of separated *CEN15* foci were seen

in 0.2 M HU-treated wild-type cells (Goshima and Yanagida, 2000; Krishnan *et al.*, 2004). The majority of wild-type cells treated with the highest concentration of HU (0.3 M HU) contained one *CEN15* foci that colocalized with one SPB, suggesting either that *CEN15* had not yet replicated or that it had replicated but it had not yet established bipolar attachment (Figure 3C). Previous work has demonstrated that unreplicated monocentric minichromosomes also remain in the vicinity of one SPB (Dewar *et al.*, 2004). Thus, the ability of *CEN15* to attain bipolar attachment is not correlated with maintaining a short spindle during the DNA replication checkpoint.

Identification of HCS Genes That Rescue spc24-9 HU Lethality

To understand why Spc24 is required for viability when DNA replication is stalled, we performed an HCS screen to identify genes that, when overexpressed, could suppress the lethality of *spc24-9* cells exposed to HU. Ten genes were identified in our HCS screen (Table 1). Multiple isolates of *SPC24* and its interacting partner *SPC25* were recovered (Janke *et al.*, 2001; Wigge and Kilmartin, 2001). We also identified four genes encoding proteins that regulate spindle dynamics—MT-associated proteins Stu1 and Stu2, the kinesin-related motor protein Kip2, and a protein involved in spindle positioning called Dma1 (Roof *et al.*, 1992; Pasqualone and Huffaker, 1994; Wang and Huffaker, 1997; Fraschini *et al.*, 2004). Two protein kinases were isolated—Mck1, which has a role in chromosome segregation, and Rck2, which has a role in the osmotic stress response pathway (Neigeborn and Mitchell, 1991; Shero and Hieter, 1991; Bilsland-Marchesan *et al.*, 2000). We identified Gic1, which has roles in cell polarity and mitotic exit (Brown *et al.*, 1997; Chen *et al.*, 1997; Hofken and Schiebel, 2004). Finally, we identified the Hcm1 transcription factor, which has also been isolated in a variety of synthetic lethal screens pertaining to the cell division cycle and chromosome segregation (Zhu and Davis, 1998; Horak *et al.*, 2002; Sarin *et al.*, 2004; Montpetit *et al.*, 2005; Daniel *et al.*, 2006). Interestingly, Hcm1 has recently been shown to activate expression of spindle and chromosome segregation proteins specifically in S phase (Pramila *et al.*, 2006). None of the HCS genes were able to rescue the inviability of a *mec1* mutant on HU plates (data not shown), suggesting that they were suppressing the specific defect of *spc24-9* mutants.

HCS Rescue Occurs through Restraining Spindle Expansion

We next determined whether the HCS genes rescued *spc24-9* HU lethality by restraining spindle expansion and thus premature chromosome segregation. *spc24-9* mutants carrying the HCS rescue plasmids were synchronized in G1 phase, released into HU for 3 h, and immunofluorescence was performed to analyze chromosome segregation and spindle morphology. All of the HCS genes were able to restore a single nuclei phenotype to *spc24-9* HU-treated cells (Figure 4D). The *STU1* and *STU2* rescue clones that we identified in our screen lacked the N-terminal 97 and 252 amino acids of Stu1 and Stu2, respectively (herein referred to as *STU1ΔN* and *STU2ΔN*). We tested whether high copy full-length *STU1* or *STU2* expression plasmids were capable of rescuing *spc24-9* HU lethality. Expression of full-length *STU2* was clearly not able to rescue either the HU lethality or chromosome segregation defects of *spc24-9* mutants, suggesting that the N-terminal truncation is an important feature of the *STU2ΔN* rescue activity (Figure 4, A and D). Expression of full-length *STU1* was able to rescue *spc24-9* HU lethality and chromosome separation at levels above vector alone, but not as well as the *STU1ΔN* clone (Figure 4, A and D).

We reasoned that expression of *STU2ΔN* might be rescuing the spindle expansion defect in HU-treated *spc24-9* mutants by destabilizing MTs. Consistent with this hypothesis, the *STU2ΔN* clone lacks the TOG1 domain of Stu2, which binds tubulin heterodimers (Al-Bassam *et al.*, 2006, 2007). Previous work has shown that expression of Stu2 lacking its TOG1 domain, which still binds MTs, results in decreased mitotic spindle length and slows down anaphase spindle elongation (Al-Bassam *et al.*, 2006). We asked whether Stu2ΔN localization is similar to endogenous Stu2 by tagging Stu2ΔN with venus fluorescent protein (VFP) (which still retains its *spc24-9* HU rescue activity) and endogenous Stu2 with cyan fluorescent protein (CFP). Indeed, we found that Stu2ΔN-VFP localization overlapped with Stu2-CFP in both wild-type and *spc24-9* mutants in log phase or HU-treated cells, consistent with previous data, demonstrating that Stu2ΔTOG1-GFP still binds MT plus ends (Supplemental Figure 2; Al-Bassam *et al.*, 2006). To test whether depletion of Stu2 activity by using another mutant form of Stu2 is also capable of preventing spindle expansion in *spc24-9* cells, we combined *spc24-9* with the *stu2-10* temperature-sensitive

---

Table 1. HCS screen of *spc24-9* HU lethality

HU rescue[a]	Gene name	Open reading frame	Biological process[b]
+	*DMA1*	YHR115C	Spindle position and orientation
+	*RCK2*	YLR248W	Oxidative and osmotic stress signaling
+	*STU1* truncated[c]	YBL034C	MT dynamics
++	*GIC1*	YHR061C	Cell polarity
+++	*KIP2*	YPL155C	Mitotic spindle positioning
+++	*MCK1*	YNL307C	Mitotic and meiotic chromosome segregation
++++	*HCM1*	YCR065W	Transcription
+++++	*STU2* truncated[d]	YLR045C	MT dynamics
+++++	*SPC24*	YMR117C	Chromosome segregation
+++++	*SPC25*	YER018C	Chromosome segregation

[a] Growth of *spc24-9* mutant carrying rescue clone struck on 0.05 M HU plates at 30°C from weak (+) to strong (+++++) growth.
[b] GO Annotation from *Saccharomyces* Genome Database.
[c] The *STU1* rescue clone is missing the N-terminal 97 amino acids.
[d] The *STU2* rescue clone is missing the N-terminal 252 amino acids.
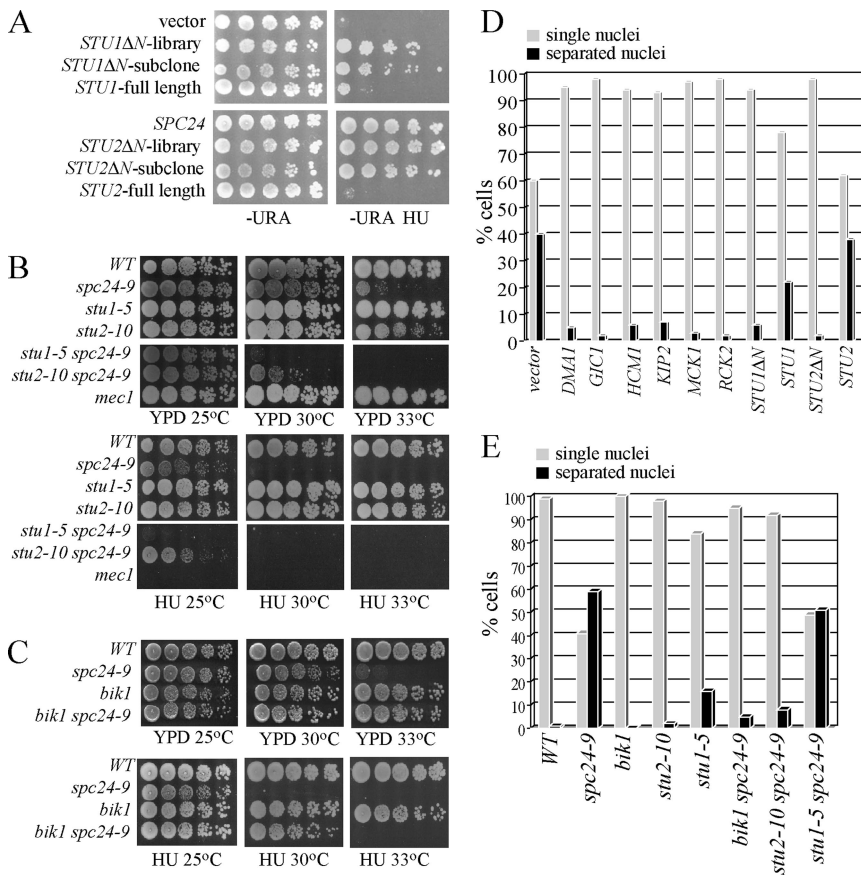
Figure 4. Spindle expansion in *spc24-9* mutants depends on active Stu2. (A) Cell dilution assay of *spc24-9* mutants carrying the 2μ plasmid vector (pRS202), *STU1ΔN*-library (HCS clone identified in screen), *STU1ΔN*-subclone (subclone of *STU1ΔN*-library containing only the *STU1* gene), *STU1* full-length (gift from T. Huffaker), full-length *SPC24*, *STU2ΔN*-library (HCS clone identified in screen), *STU2ΔN*-subclone (subclone of *STU2ΔN*-library containing only the *STU2* gene), and *STU2* full-length (gift from T. Huffaker) were grown on −URA plates at 30°C for 4 d or −URA 0.05 M HU at 30°C for 5 d. (B and C) Cell dilution assay of indicated strains grown on YPD at 25°C (2 d), 30 and 33°C (3 d), and 0.05 M HU at 25, 30, and 33°C (3 d). (D) Immunofluorescence analysis of *spc24-9* mutants carrying the indicated HCS plasmids synchronized in G1 phase with α-factor and then released into 0.2 M HU for 3 h at 30°C. Cells were counted (100 per sample) for single nuclei (gray bars) or separated nuclei (black bars) by DAPI staining. Duplicate experiments were performed with similar data, and shown is the result of one experiment. (E) Immunofluorescence analysis of indicated strains treated and analyzed as described in D.

(Ts) mutation (Severin *et al.*, 2001) and tested the double mutant for separation of nuclei upon HU treatment. Only 8% of *stu2-10 spc24-9* mutants segregated nuclei after 3 h of HU treatment compared with 59% of *spc24-9* mutants (Figure 4E). Therefore, functional Stu2 is required for the spindle expansion defect in *spc24-9* mutants. Although *stu2-10 spc24-9* double mutants maintained a short spindle during HU treatment, they were lethal on HU plates at 30°C (Figure 4B), suggesting that the defects in both Stu2 and Spc24 prevent cell cycle recovery after HU exposure.

Stu2 interacts with two other MT plus-end tracking proteins, Bim1 and Bik1 (Chen *et al.*, 1998; Lin *et al.*, 2001; Wolyniak *et al.*, 2006). Because we had previously shown that *bim1 spc24–9* mutants have a synthetic growth defect (Montpetit *et al.*, 2005), we deleted *BIK1* in *spc24-9* cells and analyzed growth phenotypes. The *bik1 spc24-9* double mutant rescued the nuclei separation defect of HU treated *spc24-9* mutants and both the HU (at 30°C) and Ts (at 33°C) lethality of *spc24-9* mutants (Figure 4, C and E). Therefore, the activity of Stu2 and Bik1 is responsible for the spindle expansion and subsequent nuclei separation and lethality of *spc24-9* cells upon HU exposure.

We also determined whether Stu1 is required for the spindle expansion activity in *spc24-9* HU-treated cells by creating a *stu1-5 spc24-9* double mutant (Yin *et al.*, 2002). The *stu1-5 spc24-9* mutant behaved in a similar manner to *spc24-9* mutants and elongated their spindles when treated with HU, suggesting that, unlike Stu2 and Bik1, Stu1 activity is not required for spindle expansion in HU exposed *spc24-9* mutants. Although both *spc24-9* and *stu1-5* individual mutants grow well at 30°C on rich media (YPD), the double mutant is synthetically lethal at 30°C (Figure 4D). In addi-

tion, the *spc24-9 stu1-5* double mutant is viable at 25°C in rich media but inviable when grown on HU plates (Figure 4D). The sensitivity of *spc24-9 stu1-5* double mutants to HU and the synthetic lethal interaction between *spc24-9* and *stu1-5* mutants suggests that Stu1 and Spc24 have a joint or parallel role in restraining spindle expansion during the DNA replication checkpoint.

Stu1 Localizes to Kinetochores before Anaphase

Stu1, which was originally isolated as a suppressor of a *tub2* (β-tubulin) mutation, interacts with Tub2 and localizes to the spindle midzone in anaphase spindles (Pasqualone and Huffaker, 1994; Yin *et al.*, 2002). However, the localization of Stu1 in relation to a SPB marker has not been assessed. We imaged Stu1 fused to VFP in relation to the Spc29-CFP SPB protein by synchronizing cells in G1 phase with mating pheromone and then releasing them into the cell cycle and fixing cells every 30 min. The budding yeast spindle reaches a length of 1.5–2 μm before entering anaphase (Pearson *et al.*, 2001). Before anaphase, we detected three evenly distributed patterns of Stu1-VFP localization in fixed cells: a bilobed distribution pattern in between the Spc29-CFP foci, which is a hallmark localization pattern for a kinetochore protein (Figure 5, top row) (He *et al.*, 2001; Measday *et al.*, 2002); a single foci located closer to one of the SPBs (Figure 5, second row); and a continuous signal in between SPBs (Figure 5, third row). In agreement with previous results, we also found that Stu1-VFP localized to the midzone of anaphase spindles (Figure 5, fourth row) (Yin *et al.*, 2002). Finally, in telophase, we observed a dispersed Stu1 signal near the SPBs (Figure 5, bottom row).
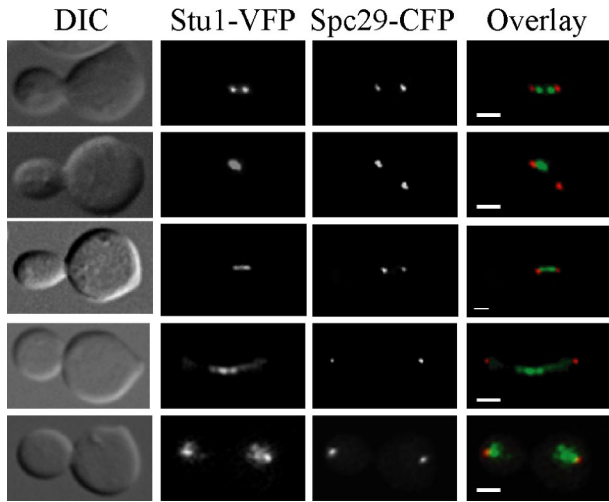
Figure 5. Stu1 localizes to kinetochores and the spindle midzone. Wild-type Stu1-VFP Spc29-CFP cells were synchronized in G1 phase with α-factor and released into the cell cycle at 30°C. Cells were fixed in 70% ethanol every 15 min for 90 min, and they were imaged as described in the *Materials and Methods*. In the overlay, green is VFP signal and red is CFP. Bar, 2 μm for all images.

Our localization data suggest that Stu1 may interact with the kinetochore. We tested whether Stu1 localizes to the kinetochore by performing Stu1-Myc ChIP assays from logarithmically growing cells. Stu1-Myc specifically associated with *CEN1* and *CEN3* DNA but not with a non-*CEN* loci, *PGK1* (Figure 6A, lane 4). We performed a Stu1-Myc ChIP assay in a *spc24-9* mutant strain at both permissive (25°C) and restrictive (37°C) temperature (Figure 6B). Stu1-Myc is still able to associate with *CEN* DNA at restrictive temperature, suggesting that Stu1 does not require Spc24 to bind kinetochores (Figure 6B, lane 4). In summary, our localization and ChIP data demonstrate that Stu1 localizes to kinetochores early in the cell cycle in an Spc24-independent manner and that it relocalizes to the spindle around the time of the metaphase to anaphase transition.

Stu2 Localizes to Kinetochores Early in the Cell Cycle

In anaphase cells, Stu2-GFP localizes to the cytoplasmic side of the SPB and along the spindle MTs as determined by immunoelectron microscopy (Kosco *et al.*, 2001). In addition, Stu2 has been shown to colocalize with kinetochores and SPBs and to bind *CEN* DNA in metaphase cells (He *et al.*, 2001). We analyzed Stu2-VFP localization in short (<1.5-μm) spindles (acquired at the time of bud emergence) and during normal spindle expansion by using time-lapse microscopy (Supplemental Figure 3). We observed that Stu2-VFP signal displayed a bilobed pattern between Spc29-CFP foci in short spindles (Supplemental Figure 3, image 10b). Time-lapse microscopy using longer exposures (which saturate Stu2-VFP spindle fluorescence) revealed that Stu2-VFP also tracks on astral microtubules and transiently associates with SPBs as astral MT shorten (data not shown). Our imaging data are consistent with Stu2 localizing primarily to kinetochores and/or the nuclear spindle before metaphase. Once spindles had lengthened (>2 μm), we detected colocalization of Stu2-VFP with Spc29-CFP as well as Stu2-VFP at the spindle midzone as described previously (Supplemental Figure 3, image 0c) (He *et al.*, 2001; Kosco *et al.*, 2001). The localization of Stu2 to kinetochores early in the cell cycle suggests that defects in kinetochore function when DNA replication is stalled by HU treatment may significantly affect Stu2 activity.

Stu2 Is Mislocalized in HU-treated spc24-9 Cells

We tested whether Stu2 localization to the kinetochore depends on functional Spc24 by using both ChIP and microscopy analyses. Stu2-Myc displayed a decreased ability to interact with *CEN* DNA in *spc24-9* cells as we increased the temperature from permissive (25°C) to semipermissive (30°C) conditions (Figure 6D, lanes 8 and 10). Stu2-Myc did not coprecipitate with *CEN* DNA in *spc24-9* mutants shifted to restrictive temperature (37°C), suggesting that Stu2 requires Spc24 to interact with the kinetochore (Figure 6D, lane 12). Although Stu2 requires Spc24 for proper *CEN* localization in logarithmically growing cells, this does not necessarily reflect the situation when cells are exposed to HU. We performed a Stu2-Myc ChIP assay in wild-type and *spc24-9* cells after treating cells with HU for 3 h at 30°C. Stu2 interaction with *CEN* DNA was highly reduced in *spc24-9* mutants compared with wild-type cells (Figure 6C, compare lanes 2 and 4). Thus, Spc24 is required for Stu2 to efficiently interact with *CEN* DNA in both log phase and HU-treated cells. To test whether Stu2 localization is perturbed in *spc24-9* cells, we performed a quantitative analysis of Stu2-VFP fluorescence during HU exposure. Cells were released from a G1 pheromone block into HU at 25°C,

Figure 6. Stu2 *CEN* binding is abolished in *spc24-9* mutants, whereas Stu1 is still able to associate with *CEN* DNA. Multiplex PCR analysis of *CEN1*, *PGK1*, and *CEN3* loci was performed with total chromatin (T) or immunoprecipitate (IP) as PCR templates. Strains were grown at 25°C to log phase and then either kept at 25°C or incubated at 30 or 37°C for 3 h. (A) Wild-type log phase cells grown at 30°C and carrying no epitope tag (No Tag; lanes 1 and 2), Stu1-Myc (lanes 3 and 4), and Stu2-Myc (lanes 5 and 6). (B) *spc24-9* mutants carrying Stu1-Myc (lanes 1–4) and a wild-type strain with no tag at 37°C (lanes 5 and 6). (C) Stu2-Myc in a wild-type (lanes 1 and 2), *spc24-9* (lanes 3 and 4), and an untagged wild-type strain (No Tag; lanes 5 and 6). (D) Stu2-Myc in a wild-type (lanes 1–6) and *spc24-9* (lanes 7–12) strains. No Tag strain (lanes 13–18) is an untagged wild-type strain. For all ChIP assays where the *spc24-9* mutant was used, we included both a wild-type and *spc24-9* untagged control, and we saw similar results; thus, only the wild-type untagged control is presented.

grown to log phase at 25°C, HU was added to a final concentration of 0.2 M HU, and cells were shifted to 30°C for 3 h. (D) Stu2-Myc in a wild-type (lanes 1–6) and *spc24-9* (lanes 7–12) strains. No Tag strain (lanes 13–18) is an untagged wild-type strain. For all ChIP assays where the *spc24-9* mutant was used, we included both a wild-type and *spc24-9* untagged control, and we saw similar results; thus, only the wild-type untagged control is presented.
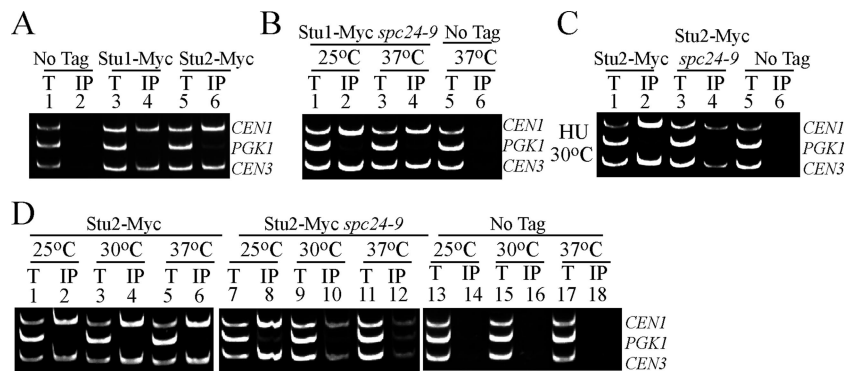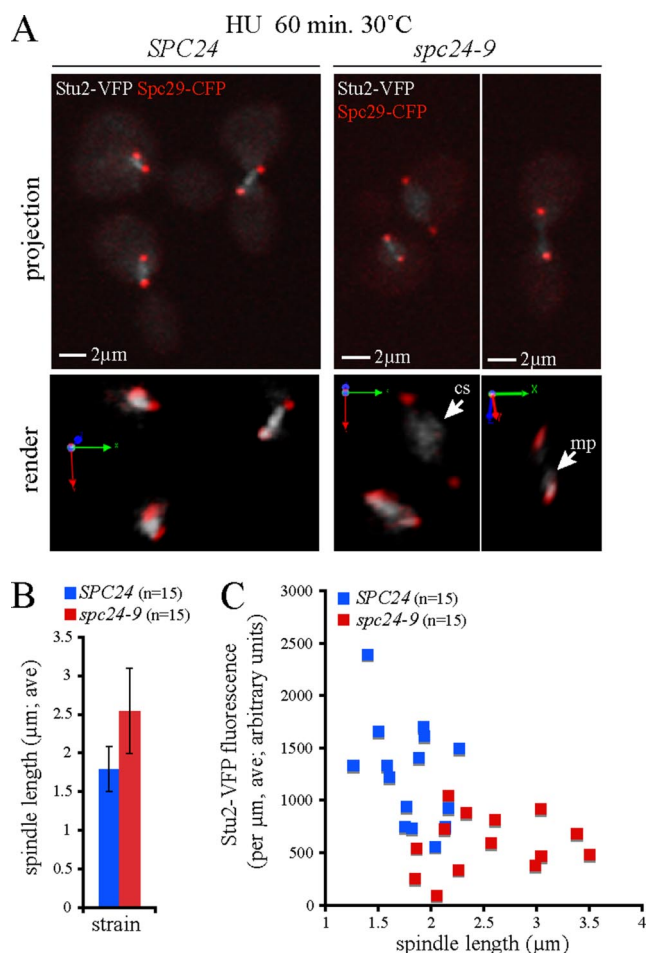
Figure 7. Increased spindle length correlates with Stu2 mislocalization and reduction. Wild-type (*SPC24*) and *spc24-9* cells expressing Stu2-VFP Spc29-CFP were synchronized in G1 phase with pheromone, released into 0.2 M HU at 25°C for 1.5 h, and shifted to 30°C in HU for 60 min, and then fixed. (A) Representative images (extended focus and three-dimensional render) of Stu2-VFP (gray scale) and Spc29-CFP (red) fluorescence in wild-type and *spc24-9* cells at 60 min after shift to 30°C are shown; mp indicates monopolar localization (near the SPB), whereas cs indicates localization to the central spindle. (B) Average (ave) spindle length of wild-type (*SPC24*) and *spc24-9* cells after a 60-min incubation in 0.2 M HU at 30°C (n = 15). (C) Quantitative analysis of Stu2-VFP fluorescence per micrometer plotted as a function of spindle length.

shifted to 30°C, and fixed after 60 min of incubation. At this time point, spindle expansion had clearly begun in *spc24-9* cells as spindle lengths averaged 2.5 μm in mutant cells compared with 1.8 μm in wild-type cells (Figure 7B). Analysis of individual cells revealed that Stu2 remained as bilobed foci in wild-type cells, whereas Stu2 signal was clearly mislocalized along the spindle midzone (cs) or next to one pole (monopolar) in *spc24-9* cells (Figure 7A, three-dimensional render, rotated). Analysis of Stu2-VFP fluorescence on the spindle indicated that Stu2-VFP fluorescence intensity decreased significantly in the *spc24-9* mutant relative to wild type (Figure 7C). Stu2-VFP also redistributed from discrete foci to diffuse fluorescence along the length of the spindle (Figure 7A); thus, Stu2-VFP fluorescence on the spindle per unit length (micrometers; see *Materials and Methods* for details) was used for the comparison of Stu2-VFP in wild-type versus *spc24-9* cells. In general, this analysis revealed that

spindles in the *spc24-9* mutant had decreased Stu2-VFP fluorescence and were longer, suggesting that spindle expansion correlates with mislocalization of Stu2 (Figure 7C). However, we noticed that low levels of Stu2-VFP fluorescence were found on both long and short spindles in *spc24-9* cells, suggesting that the relationship between spindle length and Stu2 levels was not absolute. More specifically, we wondered whether the observed spindle expansion observed in *spc24-9* cells was permanent or represented oscillations in spindle length.

To further explore the dynamics of Stu2 interaction with the spindle and spindle expansion, we analyzed dynamic changes in Stu2-VFP fluorescence and spindle length in living cells using time-lapse microscopy. For this analysis, HU-arrested wild-type and *spc24-9* mutant cells were shifted to 30°C on the microscope stage, and the HU arrest was maintained throughout the time lapse by mounting the cells in FP medium supplemented with HU. This analysis revealed that spindle length remains relatively static in wild-type cells, with an average net change (either shrinking or elongating) in length of 0.40 ± 0.125 μm during the time lapse for all cells (n = 4) analyzed (Figure 8, A and C). Spindle length at the start of the time lapse was not significantly different between wild-type and *spc24-9* cells, and it was similarly static in *spc24-9* cells (n = 4 cells/strain) during the first 5 min of the time lapse (Figure 8B). In contrast with wild-type cells, spindle length increased significantly (1.45 ± 0.638 μm) in the *spc24-9* mutant over time (Figure 8, B and C). At 18 min after the shift to 30°C, a net increase in spindle length occurred in all four *spc24-9* cells; in each cell spindle length had increased (0.9–2.3 μm; mean length increase of 1.3 ± 0.66 μm) relative to the length at the start of the time lapse and relative to all four wild-type cells (Figure 8, B and D). Thus, we chose to compare the intensity of Stu2-VFP fluorescence on the spindle at time 0 and at 18 min. Stu2-VFP fluorescence was significantly decreased in *spc24-9* cells compared with wild-type cells (Figure 8E), suggesting that mislocalization of Stu2 is correlated with the spindle expansion observed (Figure 8D). Finally, we detected significant oscillation of spindle length between 10 and 28 min in *spc24-9* cells (Figure 8B), suggesting that mislocalization of Stu2 results in transient spindle expansion. The transient nature of this defect is consistent with our observation of a subpopulation of *spc24-9* cells with short spindles and mislocalized or low Stu2-VFP levels.

DISCUSSION

The kinetochore is required to restrain spindle expansion in budding yeast when DNA replication is stalled; however, the mechanism by which kinetochores maintain spindle length in this state is not well understood. We identified genes that when overexpressed, rescue the lethality and spindle expansion defects of the *spc24-9* kinetochore mutant when exposed to HU. Two MT plus-end binding proteins, the CLASP-related protein Stu1 and XMAP215 homologue Stu2, were identified, and their interactions with the kinetochore were explored further. We find that Stu1 localizes to kinetochores early in the cell cycle and relocalizes to the spindle midzone after metaphase and that Stu2 binds to the kinetochore in a Spc24-dependent manner. In addition, inappropriate spindle expansion in HU treated *spc24-9* cells can be prevented by inhibiting Stu2 activity. We propose that mislocalization of Stu2 in *spc24-9* cells enables spindle expansion during the DNA replication checkpoint.
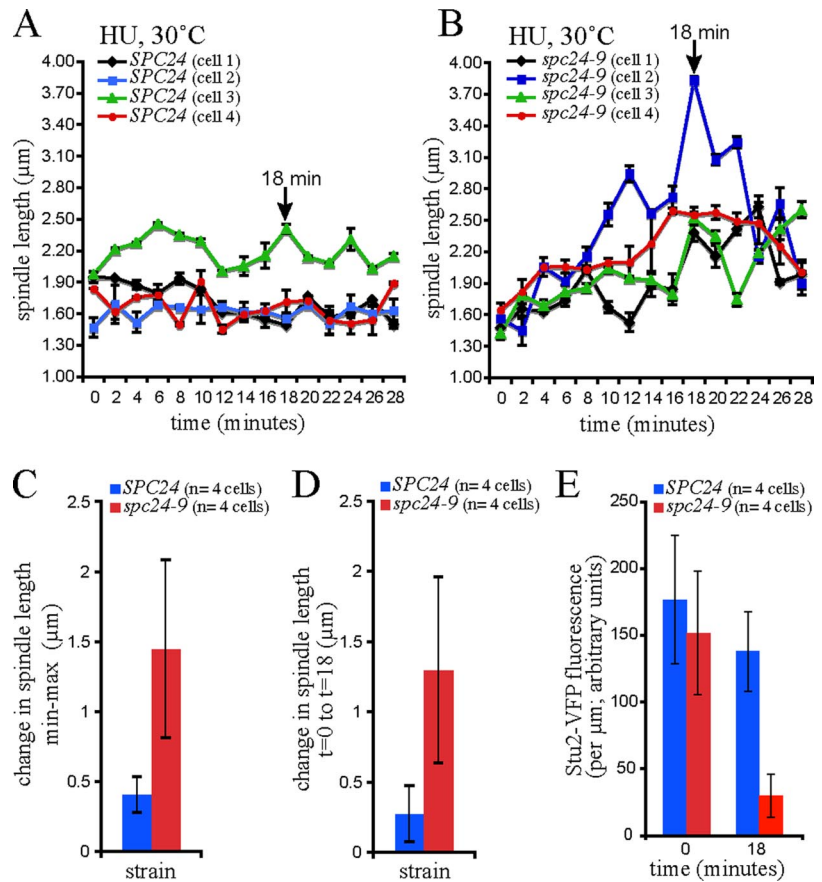
Figure 8. Decreased Stu2 in the *spc24-9* mutant results in oscillation of spindle length. Wild-type (*SPC24*) and *spc24-9* cells carrying Stu2-VFP Spc29-CFP were synchronized in G1 phase with pheromone, released into 0.2 M HU at 25°C for 1.5 h, mounted in FP supplemented with HU, shifted to 30°C on a heated stage, and time-lapse microscopy was performed. Time zero is time in HU at 30°C after equilibration on the stage at 30°C for 15 min. Spindle length is plotted for four cells of each strain (A, *SPC24*; B, *spc24-9*) as a function of time, each depicted with a different color, and shows oscillation with a net increase in length observed in all four *spc24-9* cells at 18 min. (C) In contrast with wild-type cells, spindle length increases in *spc24-9* cells. (D) Spindle length is significantly increased in all four *spc24-9* cells at 18 min relative to length at t = 0. (E) At 18 min, Stu2-VFP fluorescence on the spindle is significantly decreased in all *spc24-9* mutant cells relative to wild-type cells.

Kinetochore–MT Bipolar Attachment and the DNA Replication Checkpoint

DNA microarray studies have suggested that most *CENs* are replicated upon exposure to HU (Yabuki *et al.*, 2002; Feng *et al.*, 2006). Thus, budding yeast *CENs* may be capable of attaining bipolar attachment during HU treatment. However, our data suggest that bipolar attachment may not be the only mechanism by which kinetochores maintain short spindles during HU arrest. First, wild-type and *spc24-9* cells display similar percentages of *CEN15*-GFP bipolar foci when treated with different concentrations of HU, yet only *spc24-9* spindles expand (Figure 3B). Second, when wild-type cells are treated with high concentrations of HU, we detect a single *CEN15*-GFP focus that clearly colocalizes with one SPB (Figure 3C). These data are similar to previous studies demonstrating that a GFP-marked, unreplicated minichromosome colocalizes with one SPB after SPB separation (Dewar *et al.*, 2004). Although our data do not distinguish between replicated and unreplicated *CEN15*, *CEN15* is clearly attached to one pole, yet the spindle remains short. Thus, we propose that the ability to attain bipolar attachment during HU treatment is not correlated with restraining spindle expansion.

Stu2 Activity Enables Spindle Expansion in spc24-9 HU-treated Cells

We isolated a truncated version of the XMAP215 homologue *STU2* (*STU2ΔN*), in our *spc24-9* HCS screen that lacks the N-terminal 252 amino acids of Stu2 (Table 1). We propose that overexpression of *STU2ΔN* rescues *spc24-9* HU lethality by restraining MT dynamics induced by mislocalization of Stu2. *STU2ΔN* lacks the N-terminal TOG1 domain that binds

tubulin heterodimers but retains the TOG2 domain that binds MT plus ends (Al-Bassam *et al.*, 2006). Previous studies have shown that Stu2 lacking its TOG1 domain binds MT plus ends but cannot promote plus-end MT growth, suggesting that *STU2ΔN* inhibits *spc24-9* HU spindle expansion via the same mechanism (Al-Bassam *et al.*, 2006). The *spc24-9* mutant and the resultant mislocalization of Stu2 (see next section) is an important feature of *STU2ΔN*'s rescue function, because overexpression of *STU2ΔN* does not inhibit spindle expansion in a wild-type cell cycle (Supplemental Figure 4). Another possible Stu2ΔN rescue mechanism, which is not mutually exclusive with the previous mechanism, is that overexpression of *STU2ΔN* is titrating out a Stu2-interacting protein that is mediating spindle expansion in *spc24-9* HU cells. Stu2 interacts with the CLIP-170 orthologue Bik1 at the C terminus of Stu2 (Wolyniak *et al.*, 2006). We find that deletion of the Stu2-interacting protein Bik1 rescues the *spc24-9* spindle expansion defects and HU lethality at 30°C and that the *bik1 spc24-9* double mutant grows at a higher temperature than the *spc24-9* mutant alone (Figure 4, C and E). Thus, inhibition of Stu2 or Bik1 plus-end MT activity prevents spindle expansion when *spc24-9* mutants are under HU arrest.

Stu2 Retention at the Kinetochore Is Important for Maintaining a Short Spindle when DNA Replication is Stalled

Our data suggest that Stu2 activity is required for spindle expansion in *spc24-9* HU-treated cells. The *stu2-10 spc24-9* double mutant no longer displays inappropriate spindle expansion when exposed to HU (Figure 4E). Why is Stu2 able to promote spindle expansion in HU-treated *spc24-9*

cells but not wild-type cells? We propose that the inability to recruit and retain Stu2 at the kinetochore in *spc24-9* mutants enables Stu2 to promote MT dynamics. Our ChIP data suggest that the interaction of Stu2 with *CEN* DNA is perturbed in *spc24-9* mutants both in log phase cells and during HU treatment (Figure 6, C and D). In agreement with our studies, Stu2 does not associate with *CEN* DNA at restrictive temperature in an *ndc80-1* Ts mutant (He *et al*., 2001). Thus, the Ndc80 complex is required for recruitment of Stu2 to the kinetochore. We performed a detailed analysis of Stu2-VFP fluorescence and spindle length in both live and fixed *spc24-9* HU-treated cells. Shortly after shift to restrictive temperature (30°C for *spc24-9* cells exposed to HU), we detected spindle expansion and mislocalization of Stu2-VFP as well as its diffusion along the axis of the spindle (Figure 7). Stu2-VFP also displayed variable localization patterns including movement to one pole and to the spindle midzone in these cells (Figure 7A). Our time-lapse analysis revealed that HU treatment induces *spc24-9* mutants to undergo oscillations in spindle length, unlike in wild-type cells where relatively little change in spindle length is detected (Figure 8). We identified a window of time when the spindle was at an average maximum length in these analyses, and we quantitated Stu2-VFP fluorescence levels at this time. Stu2-VFP fluorescence was significantly reduced compared with wild-type cells, suggesting a correlation between reduction in Stu2-VFP fluorescence and spindle expansion (Figure 8E). The oscillations observed also explain why short spindles with decreased Stu2 are observed in populations of *spc24-9* cells. Finally, oscillations in spindle length were also detected in HU-exposed *rad53* mutants, suggesting that activation of the DNA replication checkpoint regulates spindle dynamics, and in the absence of the checkpoint, this restraint is compromised (Bachant *et al*., 2005). Our studies have uncovered the role of an effector of the checkpoint, Stu2, in restraining spindle dynamics while localized at the kinetochore.

The Role of Stu2 during the DNA Replication Checkpoint

Does Spc24 participate in regulating spindle expansion only during the DNA replication checkpoint or also during an unperturbed cell cycle? To address this question, we measured spindle length in a wild-type versus *spc24-9* mutant after release from a G1 block to restrictive temperature (Supplemental Figure 5). We found that early in the cell cycle, *spc24-9* mutants had longer spindles than wild-type cells consistent with a defect in the S phase checkpoint during a normal cell cycle. As cells progressed, *spc24-9* spindle expansion lagged behind wild-type cells, suggesting a delay in anaphase. These data are consistent with our analysis of DNA content during a synchronous cell cycle at restrictive temperature, which demonstrated that *spc24-9* cells progress more rapidly through S phase than wild-type cells (compare 60-min time point between wild-type and *spc24-9*; Supplemental Figure 6). However, once DNA has replicated in *spc24-9* cells, a 2N content of DNA is maintained for 2 h before 1N DNA content is once again detected (Supplemental Figure 6; Montpetit *et al*., 2005). Thus *spc24-9* cells accelerate through S phase, but are delayed in anaphase.

Mechanism of Spindle Expansion in rad53 and mec1 Mutants

The results shown here suggest that the kinetochore regulates spindle integrity during an HU-induced DNA replication checkpoint by sequestering proteins such as Stu2 that regulate MT dynamics. Why then do *mec1* and *rad53* mutants elongate their spindles during the DNA replication checkpoint? A previous study used a *CEN* transcription readthrough assay to demonstrate that the kinetochore is still capable of blocking access to the transcription machinery in a *rad53-21* strain, suggesting that the inner CBF3 kinetochore complex that binds DNA is still intact (Bachant *et al*., 2005). Ndc10, a CBF3 component, is also present on *CEN* DNA in *spc24-9* cells, suggesting that the spindle expansion is not due to defects in inner kinetochore assembly (Figure 2A). Not all central kinetochore mutants display *CEN* transcription readthrough; thus, the central kinetochore may be compromised in *rad53* or *mec1* mutant strains (Doheny *et al*., 1993). *mec1-1* HU-treated cells display upregulation of *STU2* and *CIN8* mRNA and protein levels, suggesting that increased levels of MT regulatory proteins may contribute to spindle expansion in *mec1-1* cells (Krishnan *et al*., 2004). Our data suggest that mislocalization of Stu2 by disruption of a central kinetochore complex also causes spindle expansion during the DNA replication checkpoint.

By using HU as a method to stall cells in the process of DNA replication, we have uncovered a role for the kinetochore in regulating spindle dynamics in S phase. We have discovered a role for Spc24 in recruiting Stu2 to the kinetochore to mediate MT dynamics before metaphase. Mutation of Spc24 results in mislocalization of Stu2 and deregulation of spindle dynamics when DNA replication is stalled and likely during an unperturbed S phase as well. We propose that the kinetochore regulates spindle integrity during an HU-induced DNA replication checkpoint by sequestering proteins such as Stu2 that play central roles in controlling spindle MT dynamics.

REFERENCES

Adams, I. R., and Kilmartin, J. V. (1999). Localization of core spindle pole body (SPB) components during SPB duplication in *Saccharomyces cerevisiae*. J. Cell Biol. *145*, 809–823.

Al-Bassam, J., Larsen, N. A., Hyman, A. A., and Harrison, S. C. (2007). Crystal structure of a TOG domain: conserved features of XMAP215/Dis1-family TOG domains and implications for tubulin binding. Structure *15*, 355–362.

Al-Bassam, J., van Breugel, M., Harrison, S. C., and Hyman, A. (2006). Stu2p binds tubulin and undergoes an open-to-closed conformational change. J. Cell Biol. *172*, 1009–1022.

Allen, J. B., Zhou, Z., Siede, W., Friedberg, E. C., and Elledge, S. J. (1994). The SAD1/RAD53 protein kinase controls multiple checkpoints and DNA damage-induced transcription in yeast. Genes Dev. *8*, 2401–2415.

Bachant, J., Jessen, S. R., Kavanaugh, S. E., and Fielding, C. S. (2005). The yeast S phase checkpoint enables replicating chromosomes to bi-orient and restrain spindle extension during S phase distress. J. Cell Biol. *168*, 999–1012.

Bilsland-Marchesan, E., Arino, J., Saito, H., Sunnerhagen, P., and Posas, F. (2000). Rck2 kinase is a substrate for the osmotic stress-activated mitogen-activated protein kinase Hog1. Mol. Cell Biol. *20*, 3887–3895.

Bouck, D., and Bloom, K. (2005). The role of centromere-binding factor 3 (CBF3) in spindle stability, cytokinesis, and kinetochore attachment. Biochem. Cell Biol. *83*, 696–702.

Brown, J. L., Jaquenoud, M., Gulli, M. P., Chant, J., and Peter, M. (1997). Novel Cdc42-binding proteins Gic1 and Gic2 control cell polarity in yeast. Genes Dev. *11*, 2972–2982.

Canman, C. E. (2001). Replication checkpoint: preventing mitotic catastrophe. Curr. Biol. *11*, R121–R124.

Cheeseman, I. M., Enquist-Newman, M., Muller-Reichert, T., Drubin, D. G., and Barnes, G. (2001). Mitotic spindle integrity and kinetochore function linked by the Duo1p/Dam1p complex. J. Cell Biol. *152*, 197–212.

Chen, G. C., Kim, Y. J., and Chan, C. S. (1997). The Cdc42 GTPase-associated proteins Gic1 and Gic2 are required for polarized cell growth in *Saccharomyces cerevisiae*. Genes Dev. *11*, 2958–2971.

Chen, X. P., Yin, H., and Huffaker, T. C. (1998). The yeast spindle pole body component Spc72p interacts with Stu2p and is required for proper microtubule assembly. J. Cell Biol. *141*, 1169–1179.

Clarke, D. J., Segal, M., Jensen, S., and Reed, S. I. (2001). Mec1p regulates Pds1p levels in S phase: complex coordination of DNA replication and mitosis. Nat. Cell Biol. *3*, 619–627.

Connelly, C., and Hieter, P. (1996). Budding yeast SKP1 encodes an evolutionarily conserved kinetochore protein required for cell cycle progression. Cell *86*, 275–285.

Cuschieri, L., Miller, R., and Vogel, J. (2006). γ-Tubulin is required for proper recruitment and assembly of Kar9-Bim1 complexes in budding yeast. Mol. Biol. Cell *17*, 4420–4434.

Daniel, J. A., Keyes, B. E., Ng, Y. P., Freeman, C. O., and Burke, D. J. (2006). Diverse functions of spindle assembly checkpoint genes in *Saccharomyces cerevisiae*. Genetics *172*, 53–65.

Dewar, H., Tanaka, K., Nasmyth, K., and Tanaka, T. U. (2004). Tension between two kinetochores suffices for their bi-orientation on the mitotic spindle. Nature *428*, 93–97.

Doheny, K. F., Sorger, P. K., Hyman, A. A., Tugendreich, S., Spencer, F., and Hieter, P. (1993). Identification of essential components of the *S. cerevisiae* kinetochore. Cell *73*, 761–774.

Feng, W., Collingwood, D., Boeck, M. E., Fox, L. A., Alvino, G. M., Fangman, W. L., Raghuraman, M. K., and Brewer, B. J. (2006). Genomic mapping of single-stranded DNA in hydroxyurea-challenged yeasts identifies origins of replication. Nat. Cell Biol. *8*, 148–155.

Fraschini, R., Bilotta, D., Lucchini, G., and Piatti, S. (2004). Functional characterization of Dma1 and Dma2, the budding yeast homologues of *Schizosaccharomyces pombe* Dma1 and human Chfr. Mol. Biol. Cell *15*, 3796–3810.

Gard, D. L., Becker, B. E., and Josh Romney, S. (2004). MAPping the eukaryotic tree of life: structure, function, and evolution of the MAP215/Dis1 family of microtubule-associated proteins. Int. Rev. Cytol. *239*, 179–272.

Goshima, G., and Yanagida, M. (2000). Establishing biorientation occurs with precocious separation of the sister kinetochores, but not the arms, in the early spindle of budding yeast. Cell *100*, 619–633.

Guthrie, C., and Fink, G. R. (1991). Guide to Yeast Genetics and Molecular Biology, New York: Academic Press.

Haase, S. B., and Lew, D. J. (1997). Flow cytometric analysis of DNA content in budding yeast. Methods Enzymol. *283*, 322–332.

He, X., Asthana, S., and Sorger, P. K. (2000). Transient sister chromatid separation and elastic deformation of chromosomes during mitosis in budding yeast. Cell *101*, 763–775.

He, X., Rines, D. R., Espelin, C. W., and Sorger, P. K. (2001). Molecular analysis of kinetochore-microtubule attachment in budding yeast. Cell *106*, 195–206.

Hofken, T., and Schiebel, E. (2004). Novel regulation of mitotic exit by the Cdc42 effectors Gic1 and Gic2. J. Cell Biol. *164*, 219–231.

Horak, C. E., Luscombe, N. M., Qian, J., Bertone, P., Piccirrillo, S., Gerstein, M., and Snyder, M. (2002). Complex transcriptional circuitry at the G1/S transition in *Saccharomyces cerevisiae*. Genes Dev. *16*, 3017–3033.

Hyland, K. M., Kingsbury, J., Koshland, D., and Hieter, P. (1999). Ctf19p: a novel kinetochore protein in *Saccharomyces cerevisiae* and a potential link between the kinetochore and mitotic spindle. J. Cell Biol. *145*, 15–28.

Inoue, Y. H., do Carmo Avides, M., Shiraki, M., Deak, P., Yamaguchi, M., Nishimoto, Y., Matsukage, A., and Glover, D. M. (2000). Orbit, a novel microtubule-associated protein essential for mitosis in *Drosophila melanogaster*. J. Cell Biol. *149*, 153–166.

Janke, C., Ortiz, J., Lechner, J., Shevchenko, A., Shevchenko, A., Magiera, M. M., Schramm, C., and Schiebel, E. (2001). The budding yeast proteins Spc24p and Spc25p interact with Ndc80p and Nuf2p at the kinetochore and are important for kinetochore clustering and checkpoint control. EMBO J. *20*, 777–791.

Jaspersen, S. L., and Winey, M. (2004). The budding yeast spindle pole body: structure, duplication, and function. Annu. Rev. Cell Dev. Biol. *20*, 1–28.

Kaiser, C., Michaelis, S., and Mitchell, A. (1994). Methods in Yeast Genetics, Cold Spring Harbor, NY: Cold Spring Harbor Laboratory Press.

Kolodner, R. D., Putnam, C. D., and Myung, K. (2002). Maintenance of genome stability in *Saccharomyces cerevisiae*. Science *297*, 552–557.

Kosco, K. A., Pearson, C. G., Maddox, P. S., Wang, P. J., Adams, I. R., Salmon, E. D., Bloom, K., and Huffaker, T. C. (2001). Control of microtubule dynamics by Stu2p is essential for spindle orientation and metaphase chromosome alignment in yeast. Mol. Biol. Cell *12*, 2870–2880.

Krishnan, V., Nirantar, S., Crasta, K., Cheng, A. Y., and Surana, U. (2004). DNA replication checkpoint prevents precocious chromosome segregation by regulating spindle behavior. Mol. Cell *16*, 687–700.

Krishnan, V., and Surana, U. (2005). Taming the spindle for containing the chromosomes. Cell Cycle *4*, 376–379.

Le Masson, I., Saveanu, C., Chevalier, A., Namane, A., Gobin, R., Fromont-Racine, M., Jacquier, A., and Mann, C. (2002). Spc24 interacts with Mps2 and is required for chromosome segregation, but is not implicated in spindle pole body duplication. Mol. Microbiol. *43*, 1431–1443.

Lin, H., de Carvalho, P., Kho, D., Tai, C. Y., Pierre, P., Fink, G. R., and Pellman, D. (2001). Polyploids require Bik1 for kinetochore-microtubule attachment. J. Cell Biol. *155*, 1173–1184.

Longtine, M. S., McKenzie, A., 3rd, Demarini, D. J., Shah, N. G., Wach, A., Brachat, A., Philippsen, P., and Pringle, J. R. (1998). Additional modules for versatile and economical PCR-based gene deletion and modification in *Saccharomyces cerevisiae*. Yeast *14*, 953–961.

Lopes, M., Cotta-Ramusino, C., Pellicioli, A., Liberi, G., Plevani, P., Muzi-Falconi, M., Newlon, C. S., and Foiani, M. (2001). The DNA replication checkpoint response stabilizes stalled replication forks. Nature *412*, 557–561.

McAinsh, A. D., Tytell, J. D., and Sorger, P. K. (2003). Structure, function, and regulation of budding yeast kinetochores. Annu. Rev. Cell Dev. Biol. *19*, 519–539.

Measday, V., Hailey, D. W., Pot, I., Givan, S. A., Hyland, K. M., Cagney, G., Fields, S., Davis, T. N., and Hieter, P. (2002). Ctf3p, the Mis6 budding yeast homolog, interacts with Mcm22p and Mcm16p at the yeast outer kinetochore. Genes Dev. *16*, 101–113.

Miranda, J. J., De Wulf, P., Sorger, P. K., and Harrison, S. C. (2005). The yeast DASH complex forms closed rings on microtubules. Nat. Struct. Mol. Biol. *12*, 138–143.

Montpetit, B., Thorne, K., Barrett, I., Andrews, K., Jadusingh, R., Hieter, P., and Measday, V. (2005). Genome-wide synthetic lethal screens identify an interaction between the nuclear envelope protein, Apq12p, and the kinetochore in *Saccharomyces cerevisiae*. Genetics *171*, 489–501.

Neigeborn, L., and Mitchell, A. P. (1991). The yeast MCK1 gene encodes a protein kinase homolog that activates early meiotic gene expression. Genes Dev. *5*, 533–548.

Pasqualone, D., and Huffaker, T. C. (1994). STU1, a suppressor of a beta-tubulin mutation, encodes a novel and essential component of the yeast mitotic spindle. J. Cell Biol. *127*, 1973–1984.

Pearson, C. G., Maddox, P. S., Salmon, E. D., and Bloom, K. (2001). Budding yeast chromosome structure and dynamics during mitosis. J. Cell Biol. *152*, 1255–1266.

Pinsky, B. A., Kung, C., Shokat, K. M., and Biggins, S. (2006). The Ipl1-Aurora protein kinase activates the spindle checkpoint by creating unattached kinetochores. Nat. Cell Biol. *8*, 78–83.

Pot, I., Knockleby, J., Aneliunas, V., Nguyen, T., Ah-Kye, S., Liszt, G., Snyder, M., Hieter, P., and Vogel, J. (2005). Spindle checkpoint maintenance requires Ame1 and Okp1. Cell Cycle *4*, 1448–1456.

Pot, I., Measday, V., Snydsman, B., Cagney, G., Fields, S., Davis, T. N., Muller, E. G., and Hieter, P. (2003). Chl4p and iml3p are two new members of the budding yeast outer kinetochore. Mol. Biol. Cell *14*, 460–476.

Pramila, T., Wu, W., Miles, S., Noble, W. S., and Breeden, L. L. (2006). The Forkhead transcription factor Hcm1 regulates chromosome segregation genes and fills the S-phase gap in the transcriptional circuitry of the cell cycle. Genes Dev. *20*, 2266–2278.

Roof, D. M., Meluh, P. B., and Rose, M. D. (1992). Kinesin-related proteins required for assembly of the mitotic spindle. J. Cell Biol. *118*, 95–108.

Sarin, S., Ross, K. E., Boucher, L., Green, Y., Tyers, M., and Cohen-Fix, O. (2004). Uncovering novel cell cycle players through the inactivation of securin in budding yeast. Genetics *168*, 1763–1771.

Severin, F., Habermann, B., Huffaker, T., and Hyman, T. (2001). Stu2 promotes mitotic spindle elongation in anaphase. J. Cell Biol. *153*, 435–442.

Shero, J. H., and Hieter, P. (1991). A suppressor of a centromere DNA mutation encodes a putative protein kinase (MCK1). Genes Dev. *5*, 549–560.

Shimogawa, M. M. *et al.* (2006). Mps1 phosphorylation of dam1 couples kinetochores to microtubule plus ends at metaphase. Curr. Biol. *16*, 1489–1501.

Tanaka, K., Mukae, N., Dewar, H., van Breugel, M., James, E. K., Prescott, A. R., Antony, C., and Tanaka, T. U. (2005). Molecular mechanisms of kinetochore capture by spindle microtubules. Nature *434*, 987–994.

Tytell, J. D., and Sorger, P. K. (2006). Analysis of kinesin motor function at budding yeast kinetochores. J. Cell Biol. *172*, 861–874.

Wang, P. J., and Huffaker, T. C. (1997). Stu2p: a microtubule-binding protein that is an essential component of the yeast spindle pole body. J. Cell Biol. *139*, 1271–1280.

Wei, R. R., Sorger, P. K., and Harrison, S. C. (2005). Molecular organization of the Ndc80 complex, an essential kinetochore component. Proc. Natl. Acad. Sci. USA *102*, 5363–5367.

Weinert, T. A., Kiser, G. L., and Hartwell, L. H. (1994). Mitotic checkpoint genes in budding yeast and the dependence of mitosis on DNA replication and repair. Genes Dev. *8*, 652–665.

Westermann, S., Avila-Sakar, A., Wang, H. W., Niederstrasser, H., Wong, J., Drubin, D. G., Nogales, E., and Barnes, G. (2005). Formation of a dynamic kinetochore- microtubule interface through assembly of the Dam1 ring complex. Mol. Cell *17*, 277–290.

Wigge, P. A., and Kilmartin, J. V. (2001). The Ndc80p complex from *Saccharomyces cerevisiae* contains conserved centromere components and has a function in chromosome segregation. J. Cell Biol. *152*, 349–360.

Wolyniak, M. J., Blake-Hodek, K., Kosco, K., Hwang, E., You, L., and Huffaker, T. C. (2006). The regulation of microtubule dynamics in *Saccharomyces cerevisiae* by three interacting plus-end tracking proteins. Mol. Biol. Cell *17*, 2789–2798.

Yabuki, N., Terashima, H., and Kitada, K. (2002). Mapping of early firing origins on a replication profile of budding yeast. Genes Cells *7*, 781–789.

Yin, H., You, L., Pasqualone, D., Kopski, K. M., and Huffaker, T. C. (2002). Stu1p is physically associated with beta-tubulin and is required for structural integrity of the mitotic spindle. Mol. Biol. Cell *13*, 1881–1892.

Zhu, G., and Davis, T. N. (1998). The fork head transcription factor Hcm1p participates in the regulation of SPC110, which encodes the calmodulin-binding protein in the yeast spindle pole body. Biochim. Biophys. Acta *1448*, 236–244.

Zhu, G., Muller, E. G., Amacher, S. L., Northrop, J. L., and Davis, T. N. (1993). A dosage-dependent suppressor of a temperature-sensitive calmodulin mutant encodes a protein related to the fork head family of DNA-binding proteins. Mol. Cell Biol. *13*, 1779–1787.